

Investigation of glymphatic impairment in diabetes using MRI and distributed RC line model

Esmaeil Davoodi Bojd¹, Li Zhang¹, Guangliang Ding¹, Siamak Nejad-Davarani¹, ZhengGang Zhang¹, Lian Li¹, QingJiang Li¹, Michael Chopp¹, and Quan Jiang¹

¹Neurology, Henry Ford Health System, Detroit, Michigan, United States

Introduction.

Contradict to the traditional model of cerebrospinal fluid (CSF) hydrodynamics, the glymphatic system has been recently proposed for lymphatic clearance of extracellular solutes and showing promise results in investigation of neurological diseases [1]. However, there are no reported data related to diabetes and the glymphatic system. Current study demonstrated the first investigation of glymphatic impairment after diabetes in rat using MRI. The aim of this work is to find the differences of the wasting process of contrast agent (CA) in the brain of normal and diabetic animals using contrast enhanced MRI. An equivalent electrical circuit is proposed for the glymphatic system to quantify the flow characteristics, especially waste clearance time constant, of CA.

Materials and Methods.

Image acquisition. Six rats (3 controls and 3 diabetics) followed in a CE-MRI protocol using Gd-DTPA contrast agent². T1-weighted images were acquired using a 7Tesla animal scanner with TR/TE=15/4ms and acquisition voxel size of $0.125 \times 0.167 \times 0.167 \text{ mm}^3$ and reconstructed to $0.125 \times 0.125 \times 0.125 \text{ mm}^3$. Up to 62 time volumes were acquired until 6 hours after intra-cisterna magna (ICM) contrast agent delivery. **Pre-Processing.** For each case, the non-brain tissues are masked in order to reduce the following computation time. Then, all the volumes of each case are co-registered to the first time point using rigid transformation computed in SPM8. To have a same space for comparison, we select one case as a template and register all other cases to it using a non-linear registration in SPM8. The first time point is used as the baseline for normalizing time series. **Clustering.** Since, the proposed model cannot be applied to all the voxels because of the computation complexity, first, we cluster the time series of the brain into 30 clusters using k-means clustering in MATLAB. Then, each cluster is considered as a 'site' and the average time series of that cluster is assigned to it. Moreover, by counting adjacent voxels of all pair of clusters, we build a 30by30 matrix as the 'connectivity matrix' which states 'how' a site, i , is connected to the other site, j . **Proposed model.** The CA concentration changes at time in each point of tissue is related to the tissue characteristics and also the input and output CA flow. Moreover, the concentration difference between two adjacent points causes CA to flow. Having these facts, along with correlating CA concentration and flow to electric potential and current, respectively, we can use a distributed RC line circuit as shown in Fig. 1 to model the glymphatic system. Knowing the electric potentials, V_i , $i=1\dots30$, (which are equivalent to the time series of the clusters computed from MRI images), the goal is to estimate capacitors, C_i and resistors, r_{ij} . We use a least square non-linear optimization method in MATLAB to solve the numerical differential equations describing this circuit. It should be noted that the input flow of CA is realized by an electric current source connected to the nearest site (cluster) to the injection. The estimated parameters can be used to calculate the local time constants, τ_k , of each site (cluster) which determines the delay of clearance of the CA from the tissue. This parameter is then compared between the control and diabetic cases especially within the ventricles.

Results and Discussion.

In Fig. 2, the 3D and 2D views of clustered map of a typical case is shown based on the rising time of the time series. The injection region (posterior of the brain) and the paravascular pathways are visibly distinguishable. The quantitative values of RC parameter for ventricles are shown in Table 1 for three diabetic and three normal rats. It is seen that the clearance of the CA from the ventricles is significantly different between the diabetic and normal rats. This means that the CSF moves much slower in diabetic rats. To show the capability of the proposed model, a sagittal view of the RC map for a normal and a diabetic rat is shown in Fig 3. By comparing these two maps visually, it can be concluded that there are more regions in the diabetic brain than normal one in which the CA stays longer.

Conclusion.

In this work for the first time the effect of waste clearance system in the brain was investigated in diabetes. The proposed model for describing glymphatic system can be used to identify which part of the glymphatic system is affected by diabetes. Moreover, one of the important application of the proposed approach is to determine quantitatively the effect of treatment after neurological disorder, such as diabetes.

References.

- Iliff JJ, Wang M, et al. A paravascular pathway facilitates CSF flow through the brain parenchyma and the clearance of interstitial solutes, including amyloid beta. *Science translational medicine*. 2012;4(147):147ra1; 366:576-578.
- Iliff JJ, Lee H, et al. Brain-wide pathway for waste clearance captured by contrast-enhanced MRI. *J Clin Invest*. 2013; 123(3): 1299–1309.

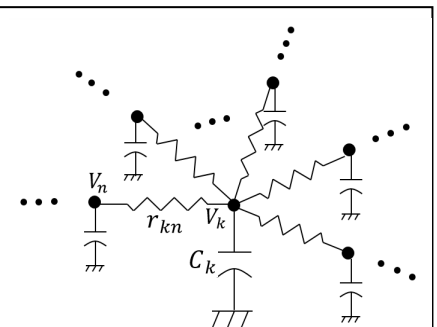


Fig 1. The proposed model for glymphatic system. $V_i, i=1\dots30$ are the electric potential which are set to the measured CA concentrations from MRI. Then, the circuit parameters are estimated using a numerical optimization method.

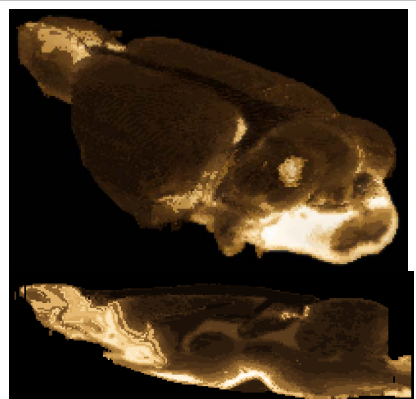


Fig 2. 3D (top) and 2D (bottom) views of clustered map of a typical case. The clusters are sorted based on the rising time of time series. The brighter, the sooner CA reaches into.

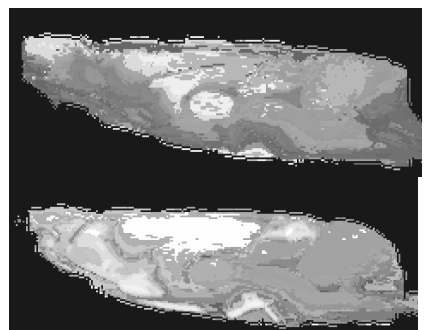


Fig 3. The RC map of a normal (top) and a diabetic (bottom) brain rats. The brighter, the slower clearance rate of CA.

Table 1. The mean and STD values of RC parameter in the ventricles of diabetic (D) and normal (N) rats.

	RC value (min)
D1	504.1 \pm 84.1
D2	950.2 \pm 108.2
D3	492.2 \pm 62.4
N1	135.6 \pm 21.1
N2	160.5 \pm 18.3
N3	115.8 \pm 27.5